Understanding Fivefold Symmetry in Electron-Diffraction Patterns

Lequan Min

School of Mathematics and Physics
University of Science and Technology Beijing, Beijing 100083, PR China

Abstract

Electron-diffraction patterns with 5-fold rotational symmetry of experimental alloy phases are assumed to be produced by periodic structures. One three-dimensional periodic structure is presented based on two kind polyhedrons. The structure can be used as one orthorhombic cell atomic model to describe the alloy phases. The Fourier-transform patterns of the model are simulated along six "symmetry directions". The chemical composition of the model is similar to that of the Al-Mn alloy phase. Details of the motivations and approaches that lead to these models are discussed. This study suggests that non classical periodic structures are also well candidates to describe quasicrystals. Further studies in this area are encouraged.
Keywords: Condensed matter physics; Electron-diffraction; 5-fold symmetry; Quasicrystal; Two kind polyhedrons; Periodic model; Fourier-transform patterns

1 Introduction

According to the classical crystallographic theory, a crystal structure can have n-fold rotational symmetry only if n = 2, 3, 4, or 6. As a consequence, the diffraction patterns of a crystal structure have only the same n-fold symmetry. The discoveries of the alloy phases with 5−, 8−, 10−, and 12−fold symmetry electron-diffraction patterns (EDPs) consisting of sharp peaks [see [1, 2, 3, 4, 5]] have broken the crystallographic restriction.

The popular point of view is that these alloy phases are a fundamentally new class of ordered atomic structures that exhibit: long-range quasiperiodic translation order, and long-range orientational order with disallowed crystallographic symmetry; or practically these phases are randomly packed (see [6]). These phases are now called quasicrystals.

The EDPs show 12-fold rotational symmetry were observed by Chen Li, and Kuo[5] in V-Ni and V-Ni-Si alloys in 1988. The group have interpreted their alloys as two-dimensional quasicrystals rather than crystals. In previous papers ([7, 8, 9]), we introduced several 3D periodic structures based on so-called $T - polyhedron$. These structures have be used as mathematical models to describe the V-Ni and V-Ni-Si alloy systems. The Fourier-transform patterns (FTPs) of the models were in good agreement with all of the corresponding EDPs of these alloys.

In previous versions of this study[10], we have reported that the high-resolution electron-microscopic (HREM) image of Mn-Al-Si taken with the incident beam parallel to the fivefold symmetry zone axis cannot be described by Penrose tiling [see Fig. 3 in Ref.[11]]; the HREM image reported by Hiraga et al. [11] has periodic characteristic formed by isolated and overlapped regular decagon [see Fig. 1]. The positions of the spots of the EDP shown 5-fold rotational symmetry can be assumed to located at integral lattice points in an orthogonal coordinate system.

After detailed studies, this paper presents an improved periodic model which can better interpret the EDPs of the five-fold QC along six "symmetery directions".

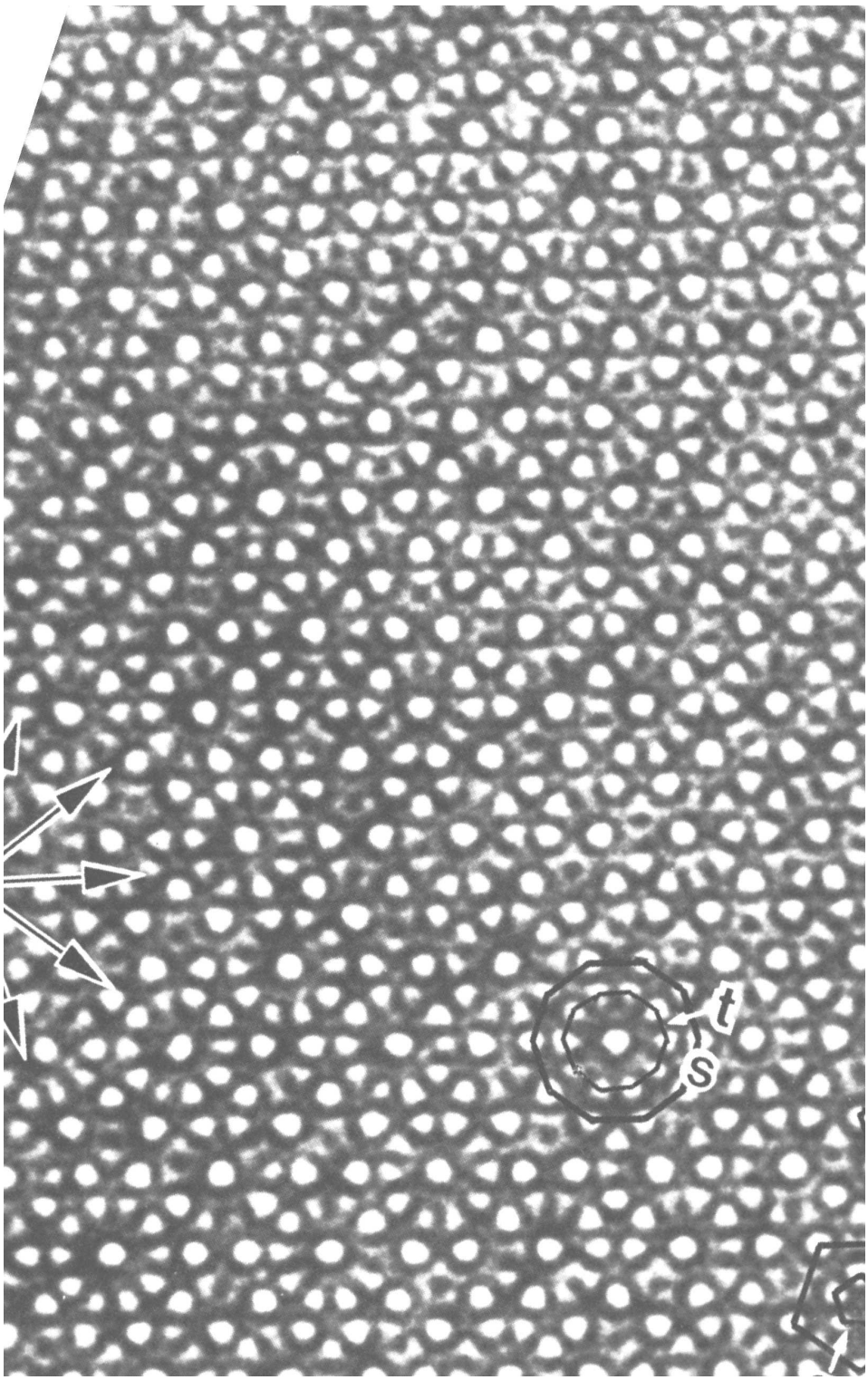

Figure 1: The HREM of Mn-Al-Si QC with the incident beam along the "five-fold symmetry" axis, showing periodic characteristic that some strong bright spots formed regular dodecagons (embedded by weak bright spots) exist in isolated way or overlapped way. [Courtesy of K. Hiraga, Tohoko Univercity. Also see Fig.2 in Ref. [11]].

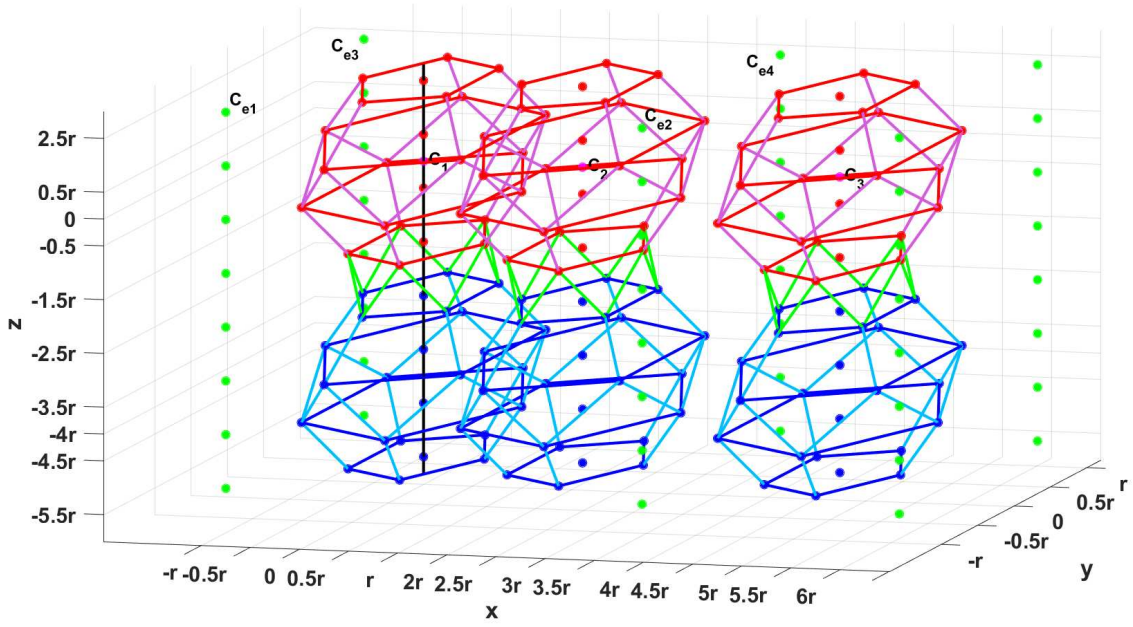

Figure 2: Each PPRP translates along $z-axis$ direction forming a polyhedron with 10 triangle faces and regular pentagon top and regular pentagon bottom [see green colored lines].

The fundamental units the model consist of isolated and overlapped polyhedrons. The features are given as follows [see Fig. 2]:

(a) Polyhedron with 12 pentagon faces whose top and bottom are regular pentagons (PPRP).

(b) Along z-axis direction, forming polyhedron with 10 triangle faces and regular pentagon top and regular pentagon bottom.

The rest of the paper is divided into three sections. Section 2 constructs the periodic mathematical model. Section 3 simulates the FTPs of the model. Finally, Sect. 4 concludes the paper.

2 Three-Dimensional Periodic Mathematical Model

The fundamental units of the model consist of isolated and overlapped PPRPs. The projection of the model on $x-y$ plan is shown in Fig. 3. In a unit cell, there are two isolated PPRPs and four overlapped PPRPs. There are 8×4 atoms surrounding the PPRPs [see $C_{e1}\sim C_{e8}$ in Figs. 3 $\sim$5].

Figure 3 is similar to the HREM images obtained by Hiraga et al. from Al-Mn-Si alloy [see Fig.1 and Fig.2 in Ref. [11]]. Therefore the model generated by orthorhombic cells.

Let r be the radius of the projection circles of the PPRPs [see Fig. 3]. The lengths of the cubic cell are given as follows:

$$|\overrightarrow{\mathbf{a}_1}| = r(5+6\sin(\pi/10)), \tag{1}$$

$$|\overrightarrow{\mathbf{a}_2}| = 4r(1+\sin(\pi/10))\cos(\pi/10), \tag{2}$$

$$|\overrightarrow{\mathbf{a}_3}| = 4r \tag{3}$$

where $\mathbf{a}_1$, $\mathbf{a}_2$ and $\mathbf{a}_3$ are primitive lattice vectors.

The positions of the twenty atoms of an PPRP with center at (0, 0, 0) are listed in Table 1. The positions of the four "centers " of an PPRP with center at (0, 0, 0) are given in Table 2.

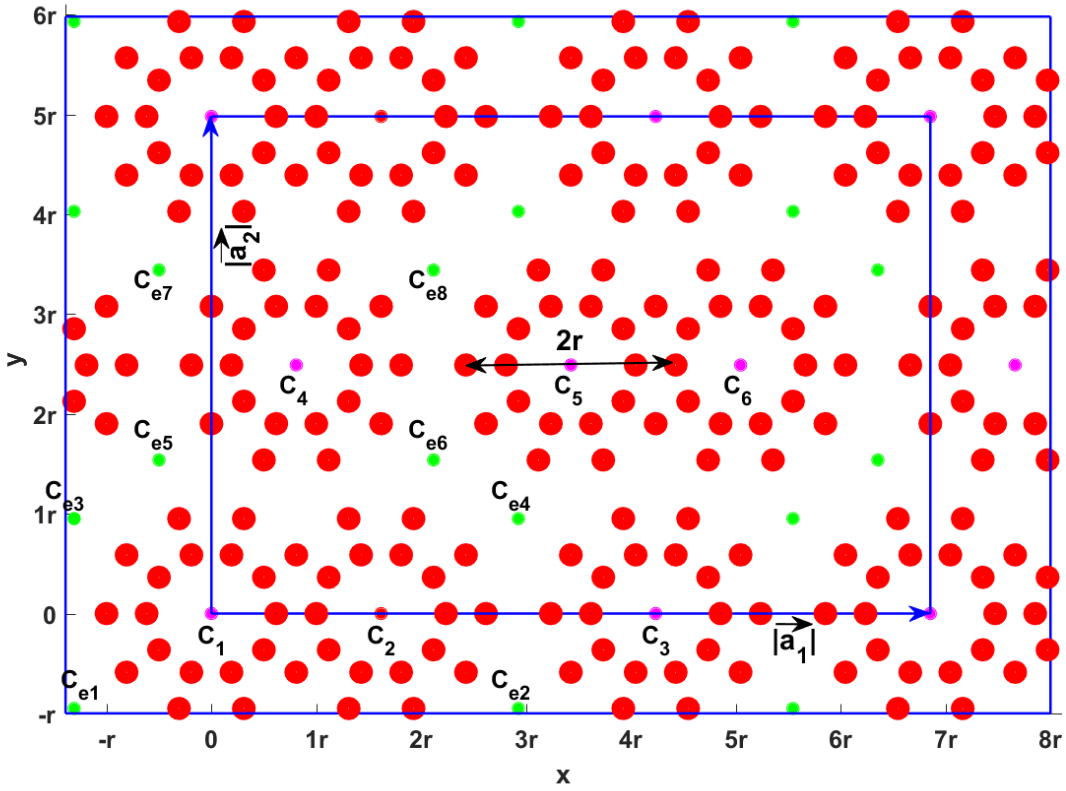

Figure 3: The formed tiling of the projection on $x-y$ plane of the periodic model.

Table 1: The positions of the twenty atoms of an PPRP with center at (0, 0, 0) where $j = 1, 2, 3, 4, 5$.

i -th type	x_j^i	y_j^i	z_j^i
1	$2r\sin(\pi/10)\cos((72\pi j+36)/180)$	$2r\sin(\pi/10)\sin(72\pi j+36/180)$	$3r/2$
2	$r\cos(72\pi j/180)$	$r\sin(72\pi j/180)$	$r/2$
3	$r\cos((72\pi j+36)/180)$	$r\sin((72\pi j+36)/180)$	$-r/2$
4	$2r\sin(\pi/10)\cos((72\pi j)/180)$	$2r\sin(\pi/10)\sin((72\pi j)/180)$	$-3r/2$

Table 2: The positions of the four "center" atoms of a PPRP with center at (0, 0, 0).

i -th type	x_0^i	y_0^i	z_0^i
1	0	0	$3r/2$
2	0	0	$r/2$
3	0	0	$-r/2$
4	0	0	$-3r/2$

Each PPRP translates $|\vec{\mathbf{a}_3}|$ along $z-axis$ direction forming a new polyhedron with 10 triangle faces, and regular pentagons on its top and bottom. The edges of the new polyhedron are the same as those of the PPRP [see Fig. 2 and Fig. 6].

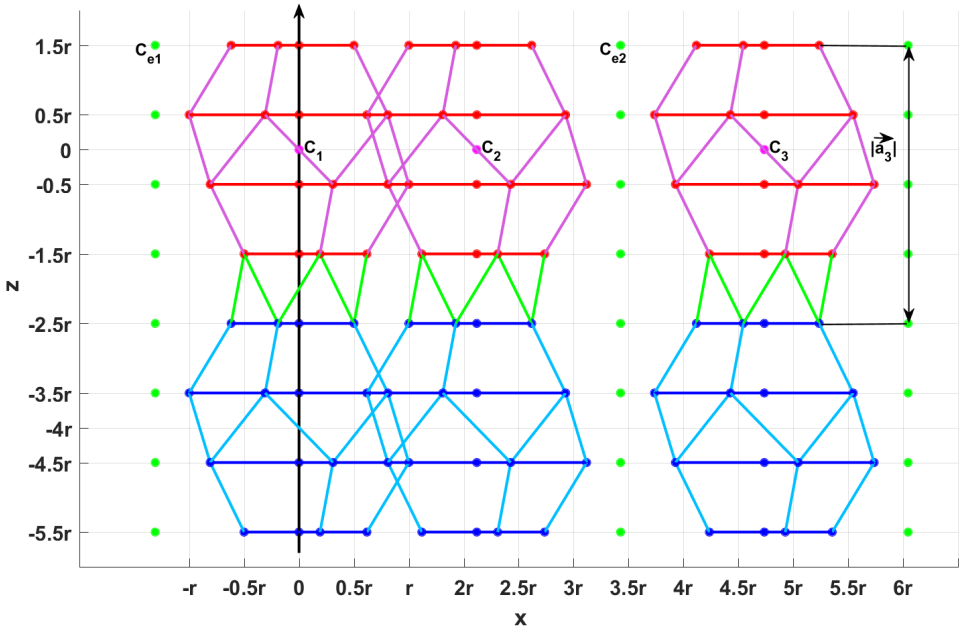

Figure 4: The projection on $x-z$ plane of one isolated PPRP and two overlapped PPRPs.

Denote C_0^i $(i=1,2,\ldots,6)$ to be the centers of the six PPRPs (denoted by $C_j, j=1,2,\ldots,6$) in a unit primitive cell [see Figs. 3 and 4]. C_0^i's have the following forms:

$$C_0^1 = (0,0,0), \tag{4}$$
$$C_0^2 = (r(1+2\sin(\pi/10)),0,0), \tag{5}$$
$$C_0^3 = C_0^2 + 2r(1+\sin(\pi/10)),0,0), \tag{6}$$
$$C_0^4 = (2r(1+\sin(\pi/10))\cos(2\pi/5), 2r(1+\sin(\pi/10))\sin(2\pi/5,0), \tag{7}$$
$$C_0^5 = C_0^4 + 2r(1+\sin(\pi/10)),0,0), \tag{8}$$
$$C_0^6 = C_0^5 + (r(1+2\sin(\pi/10)),0,0). \tag{9}$$

The the positions of the atoms of the mth PPRP can denoted by:

$$C_j^{m,i} = C_0^m + (x_j^i, y_j^i, z_j^i), \quad j=1,2,3,4,5;\ i=1,2,3,4; m=1,2,\ldots,6. \tag{10}$$

The the "center" positions of the atoms of the mth PPRP can denoted by:

$$C_0^{m,i} = C_0^m + (x_0^i, y_0^i, z_0^i), \quad i=1,2,3,4; m=1,2,\ldots,6. \tag{11}$$

The positions of the of the surrounding atoms $e_i's$ $(i=1,\ldots,8)$ have the following forms [see Fig.3-Fig.5]:

$$C_{e1} = (-r(1+2\sin(\pi/10))\cos(\pi/5), -r(1+2\sin(\pi/10))\sin(\pi/5), 3r/2) \triangleq (x_{1e}, y_{1e}, 3r/2), \tag{12}$$
$$C_{e2} = (r(1+2\sin(\pi/10)) + x_{1e}, y_{1e}) \triangleq (x_{2e}, y_{2e}, 3r/2), \tag{13}$$
$$C_{e3} = (x_{1e}, -y_{1e}, 3r/2) \triangleq (x_{3e}, y_{3e}, 3r/2), \tag{14}$$
$$C_{e4} = (x_{2e}, -y_{1e}, 3r/2) \triangleq (x_{4e}, y_{4e}), 3r/2), \tag{15}$$
$$C_{e5} = (-4r\sin(\pi/10)^2\sin(\pi/10)+1), r\sin(\pi/5)(2\sin(\pi/10)+2)3r/2) \triangleq (x_{5e}, y_{5e}, 3r/2), \tag{16}$$
$$C_{e6} = (2r(1+\sin(\pi/10))\cos(\pi/5), 2r(1+\sin(\pi/10))\sin(\pi/5)], 3r/2) \triangleq (x_{6e}, y_{6e}, 3r/2), \tag{17}$$
$$C_{e7} = (x_{6e}+x_{1e}, y_{1e}+y_{4e}) \triangleq (x_{7e}, y_{7e}, 3r/2) \tag{18}$$
$$C_{e8} = (x_{6e}, y_{7e}) \triangleq (x_{8e}, y_{8e}, 3r/2). \tag{19}$$

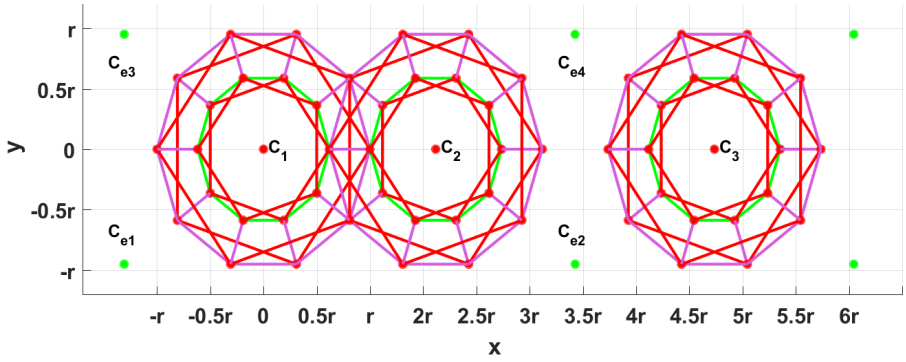

Figure 5: The projection on $x-y$ plane of one isolated PPRPs and two overlapped PPRPs.

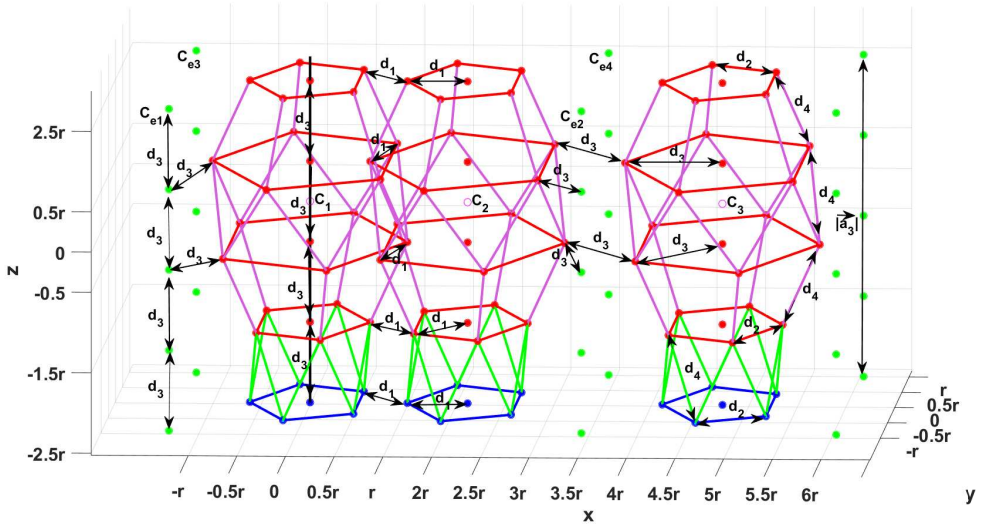

Figure 6: The distances between two neighboring atoms in the model.

The positions of the 4 atoms at $e_m\,(m=1,\ldots,8)$ along $z-axis$ direction have the forms:

$$C_e^{m,1}=(x_{me},y_{me},3r/2), \tag{20}$$
$$C_e^{m,2}=(x_{me},y_{me},r/2), \tag{21}$$
$$C_e^{m,3}=(x_{me},y_{me},-r/2), \tag{22}$$
$$C_e^{m,4}=(x_{me},y_{me},-3r/2). \tag{23}$$

In summary, we construct an orthorhombic cell model. In a unit primitive cell, there are 176 atoms. The distances between two atoms within the unit primitive cell are listed as follows [see Fig. 6]:

$$d_1=2r\sin(\pi/10)\approx 0.6180r, \tag{24}$$
$$d_2=4r\sin(\pi/10)\sin(\pi/5)\approx 0.7265r, \tag{25}$$
$$d_3=r, \tag{26}$$
$$d_4=r\sqrt{((1-2\sin(\pi/10))^2+1)}\approx 1.0705r. \tag{27}$$

3 Fourier-Transform Patterns of the Model

3.1 FTPs of the Model

Now we use the primitive lattices vector $\boldsymbol{a}_1$, $\boldsymbol{a}_2$ and $\boldsymbol{a}_3$ to express the coordinates of the atoms defined by (4)–(23).

(1) For the atoms located at the positions defined by (10)

$$C_j^{m,i} = \alpha_j^{m,i}\boldsymbol{a}_1 + \beta_j^{m,i}\boldsymbol{a}_2 + \gamma_j^{m,i}\boldsymbol{a}_3 \quad for \quad 1 \le i \le 4; \quad 1 \le j \le 5, 1 \le m \le 6. \tag{28}$$

(2) For the atoms located at the positions defined by (11)

$$C_0^{m,i} = \alpha_0^{m,i}\boldsymbol{a}_1 + \beta_0^{m,i}\boldsymbol{a}_2 + \gamma_0^{m,i}\boldsymbol{a}_3 \quad for \quad 1 \le i \le 4, 1 \le m \le 6. \tag{29}$$

(3) For the atoms located at the positions defined by (20)-(23)

$$C_e^{m,i} = \alpha_e^{m,i}\boldsymbol{a}_1 + \beta_e^{m,i}\boldsymbol{a}_2 + \gamma_e^{m,i}\boldsymbol{a}_3 \quad for \quad 1 \le i \le 4, 1 \le m \le 8. \tag{30}$$

Therefore the distribution of atoms in the model may be expressed by the function

$$\begin{aligned}\rho(\boldsymbol{r}) \quad = \quad & \sum_{h=-\infty}^{+\infty}\sum_{k=-\infty}^{+\infty}\sum_{l=-\infty}^{+\infty}\left(\sum_{i=1}^{4}\sum_{j=1}^{5}\sum_{m=1}^{6} f_{ijm}\delta(\boldsymbol{r} - (h+\alpha_j^{m,i}\boldsymbol{a}_1) + (k+\beta_j^{m,i}\boldsymbol{a}_2) + (l+\gamma_j^{m,i}\boldsymbol{a}_3)) + \right. \\ & \sum_{i=1}^{4}\sum_{m=1}^{6} f_{im}\delta(\boldsymbol{r} - (h+\alpha_0^{m,i}\boldsymbol{a}_1) + (k+\beta_0^{m,i}\boldsymbol{a}_2) + (l+\gamma_0 m, i\boldsymbol{a}_3)) + \\ & \left.\sum_{m=1}^{8}\sum_{i=1}^{4} f_{emi}\delta(\boldsymbol{r} - (h+\alpha_e^{m,i}\boldsymbol{a}_1) + (k+\beta_e^{m,i}\boldsymbol{a}_2) + (l+\gamma_e^{m,i}\boldsymbol{a}_3))\right)\end{aligned}$$

where f_{ijm},f_{im}, and f_{emi} are the scattering factors of the atoms at the positions $C_j^{m,i}$, $C_0^{m,i}$, and $C_e^{m,i}$. For the sake of simplicity, let those scattering factors equal to one.

The diffraction intensity $I(h,k,l)$ (Fourier-transform pattern) at the reciprocal-lattice point $h\boldsymbol{a}_1^* + k\mathbf{a}_2^* + l\boldsymbol{a}_3^*$ is given by

$$I(h,k,l) = \mu\left|\int_\infty^\infty\int_\infty^\infty\int_\infty^\infty \rho(\mathbf{r})exp(-i(h\boldsymbol{a}_1^* + k\mathbf{a}_2^* + l\boldsymbol{a}_3^*))dxdydz.\right|^2 \tag{31}$$

where μ is a constant. Therefore,

$$
\begin{aligned}
I(h,k,l) &= \mu \Bigg[\Bigg[\sum_{i=1}^{4} \sum_{j=1}^{5} \sum_{m=1}^{6} f_{ijm} \cos(2\pi(h\alpha_j^{mi} + k\beta_j^{mi} + l\gamma_j^{mi})) + \\
&\quad \sum_{i=1}^{4} \sum_{m=1}^{6} f_{im} \cos(2\pi(h\alpha_0^{m,i} + k\beta_0^{m,i} + l\gamma_0^{m,i})) + \\
&\quad \sum_{i=1}^{4} \sum_{m=1}^{8} f_{emi} \cos(2\pi(h\alpha_e^{m,i} + k\beta_e^{m,i} + l\gamma_e^{m,i})) \Bigg]^2 + \\
&\quad \Bigg[\sum_{i=1}^{4} \sum_{j=1}^{5} \sum_{m=1}^{6} f_{ijm} \sin(2\pi(h\alpha_j^{mi} + k\beta_j^{mi} + l\gamma_j^{mi})) + \\
&\quad \sum_{i=1}^{4} \sum_{m=1}^{6} f_{im} \sin(2\pi(h\alpha_0^{m,i} + k\beta_0^{m,i} + l\gamma_0^{m,i})) + \\
&\quad \sum_{i=1}^{4} \sum_{m=1}^{8} f_{emi} \sin(2\pi(h\alpha_e^{m,i} + k\beta_e^{m,i} + l\gamma_e^{m,i})) \Bigg]^2
\end{aligned} \tag{32}
$$

where let $\mu = 0.0009$.

The FTPs of the model along different "symmetry directions" are shown Figs. 7, 9-12. The FTPs (diffraction) spots are shown as circles whose diameters are proportional to their intensities; the spots whose intensities are less than $0.07I(0,0,0)$ are omitted.

Figure 8 shows a typical EDP of a quasicrystal with five-fold rotational symmetry [see [12]]. The FTPs shown in Figs 7 and 9 are very similar to the corresponding QC EDPs [see Fig. 8, or Fig. 2 in Ref. [1]]. The FTPs shown in Figs. 10-13 have the characteristics corresponding to the QC EDPs [see Fig.2 in Ref. [1]]. The the positions of the line connected spots shown in Figs. 10-13 are good in agreement with the positions of the corresponding strong spots shown in Fig. 2 in Ref. [1].

In addition, if let $r = 6.5\mathring{A}$, then the volume of the unit primitive cell of the model is $44.5517 \times 32.3687 \times 26\mathring{A}^3$. Formulas (23)-(25) show that the interatomic distances of the model are between $d_{min} = 2r\sin(pi/10) \approx 4.017\mathring{A}$, and $d_{max} = \sqrt{(1-2\sin(pi/10))^2+1} \approx 6.8512\mathring{A}$. Furthermore, if the Al atoms at the "centers" of the 6 PPRPs in a unit primitive cell, and the Mn atoms at the other positions. Then there are 32 Al atoms and 224 Mn atoms in a unit primitive cell. Hence the chemical composition of the model is about $Al_{13.6}Mn_{86.4}$ which is very closed to the chemical composition of five fold rotational symmetry quasicrystal [1]. Therefore the atomic structure presented here is acceptable.

In summary, the presented periodic model can generate the Fourier-transform patterns which are similar to corresponding EDPs of "5-fold symmetry" quasicrystals. The chemical composition of the model is very closed to the chemical composition of the five fold rotational symmetry quasicrystal [1].

3.2 Discussions

If the idealized EDPs of "5-fold symmetry" quasicrystals have 5-fold symmetry in a mathematical sense, then we can conclude that the HREM images of the quasicrystal imply that the quasicrystals are perturbed quasiperiodic structures.

But we can also reasonably assume that the diffraction spots in the idealized EDPs of "5-fold symmetry" quasicrystals are located at corresponding integral lattices points in an orthogonal coordinated systems [see Figs. 6, 9 and 14] which are hardly distinguishable form a pattern with 5-fold symmetry in a strict sense. This means that the "5-fold symmetry" quasicrystals are essentially crystals but not

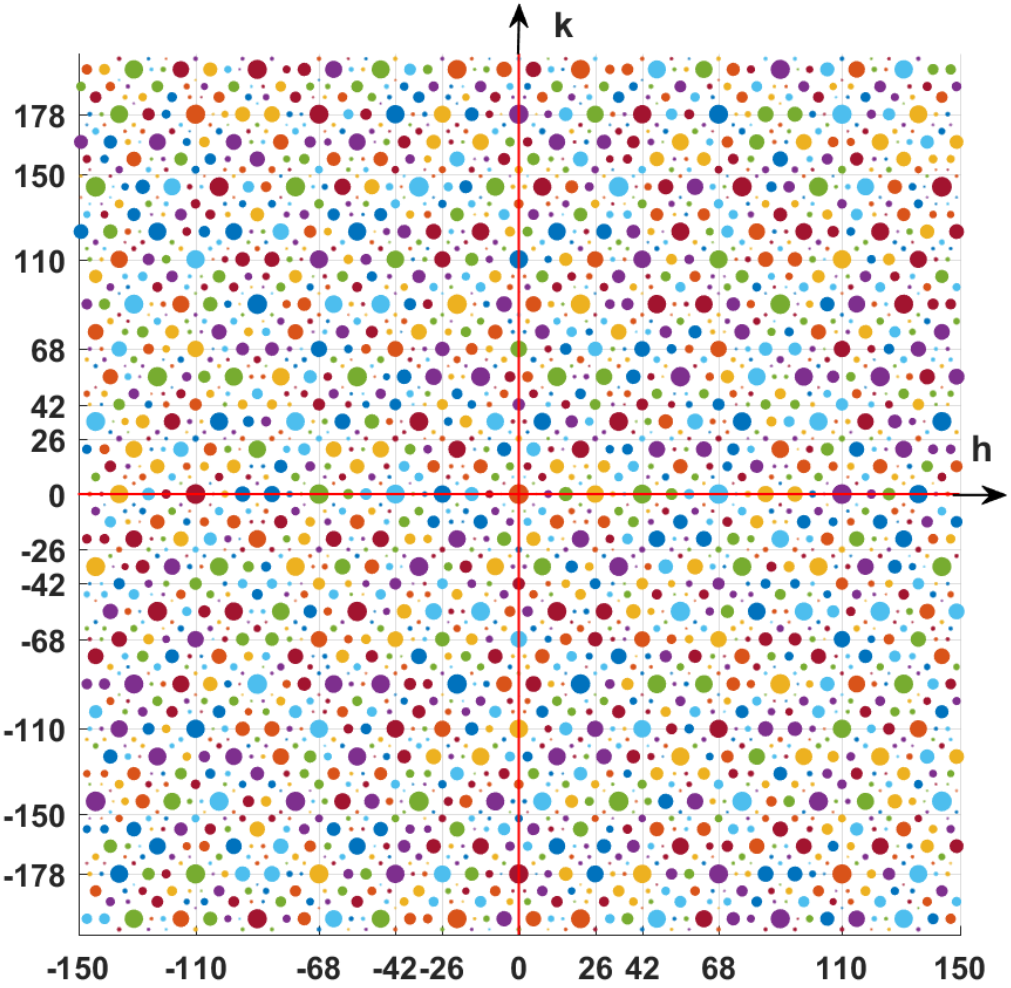

Figure 7: Fourier-transform pattern of the model in a plan orthogonal to a "5-fold symmetry axis".

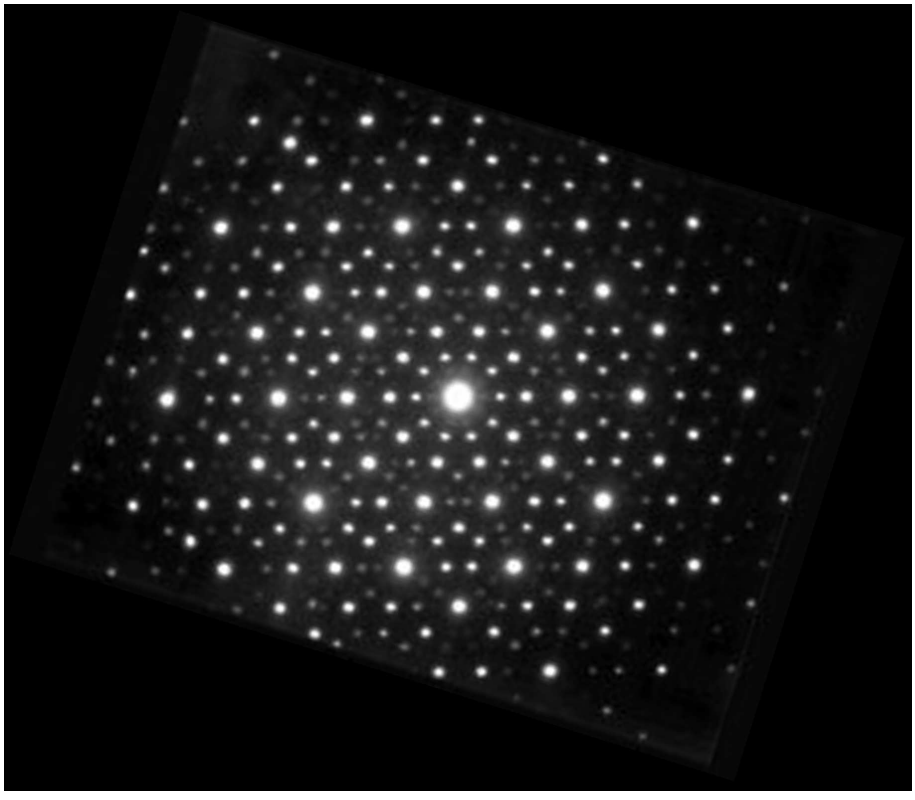

Figure 8: The digitized EDP of a quasicrystal with 5-fold rotational symmetry.

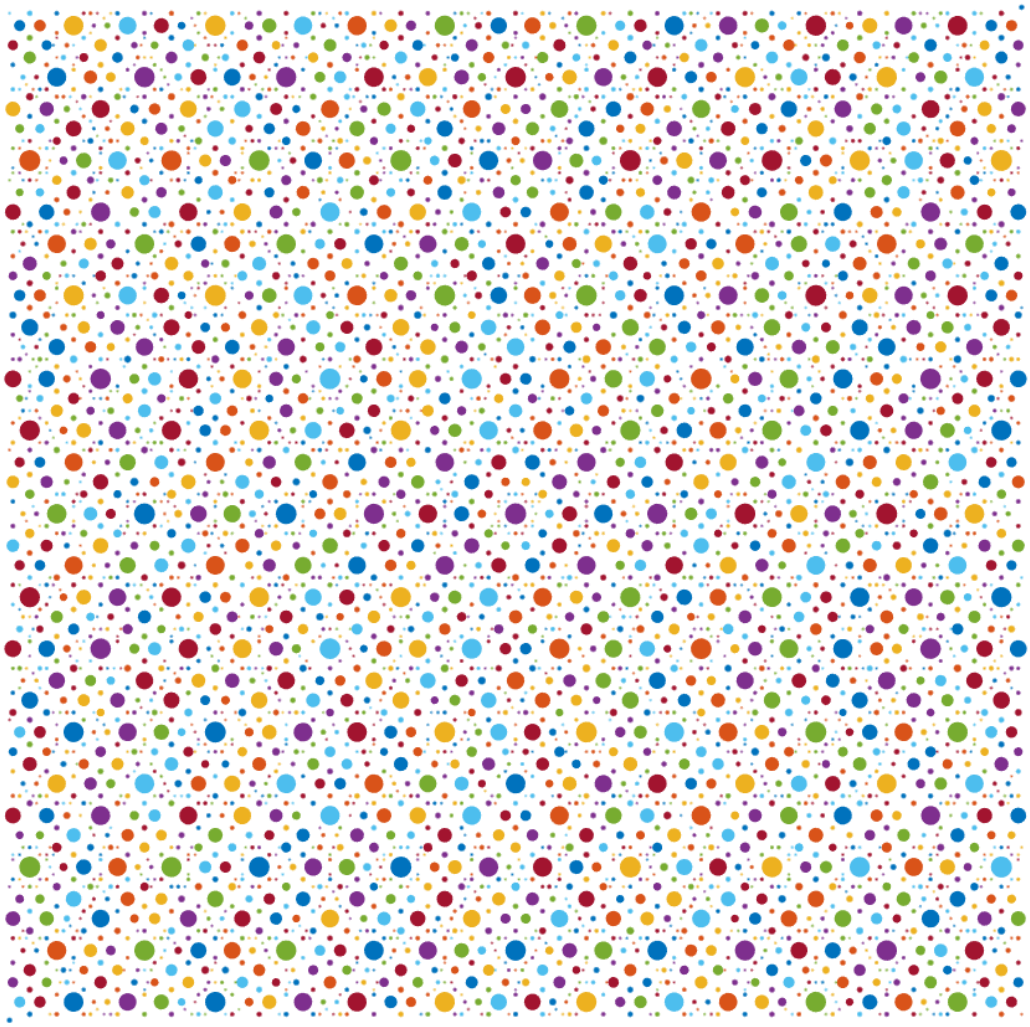

Figure 9: Fourier- transform of the new model in a plan orthogonal to a"5-fold axis" with an angle 63.43^o to $z - axis$.

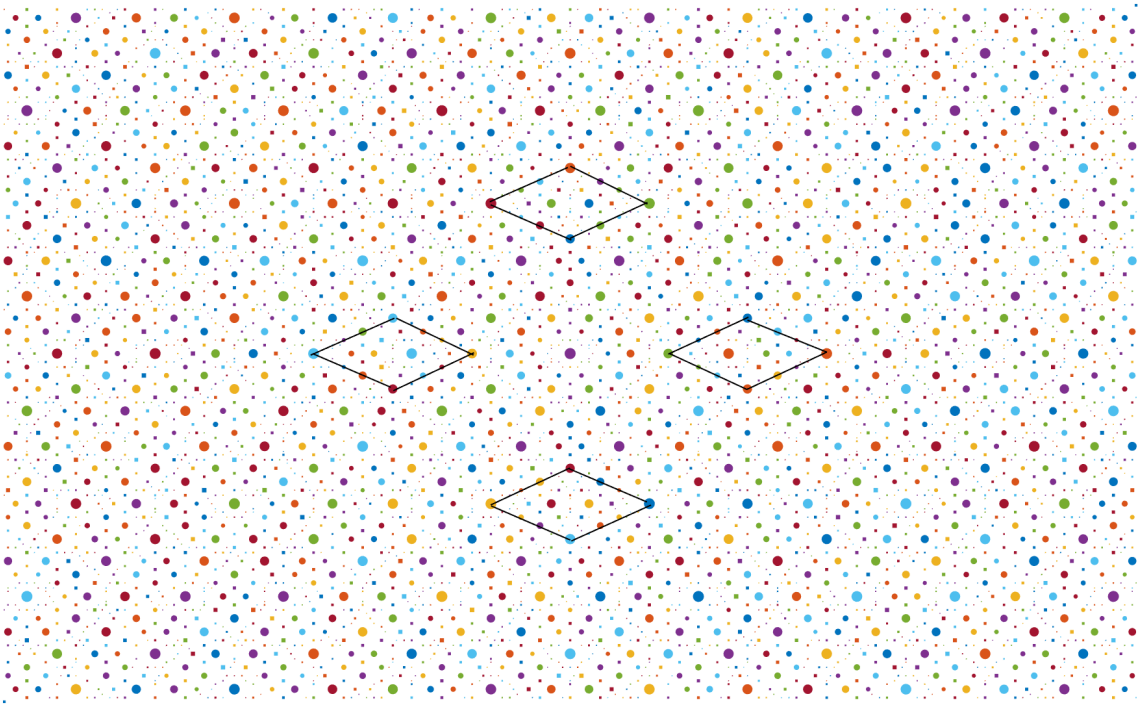

Figure 10: Fourier-transform of the new model in a plan orthogonal to a "2-fold axis" with an angle 31.72^o to $z - axis$.

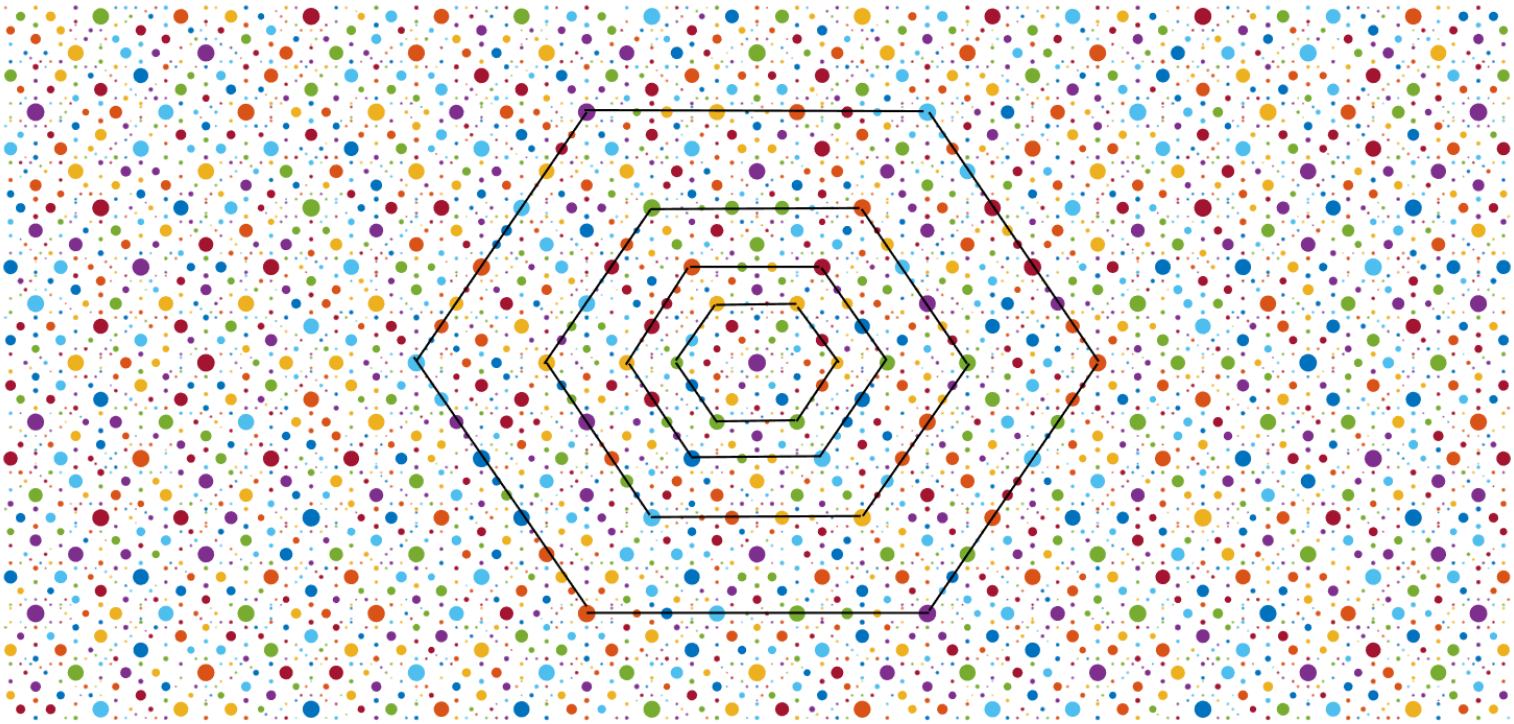

Figure 11: Fourier-transform of the new model in a plan orthogonal to a "3-fold axis" with an angle 37.38^o to $z - axis$.

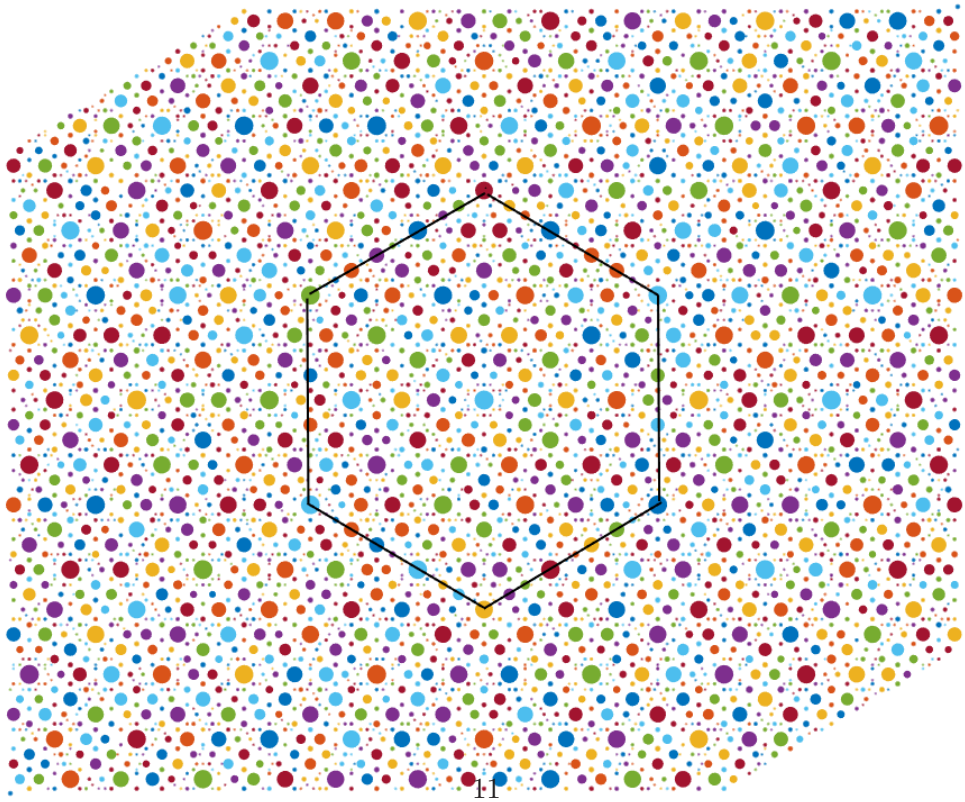

Figure 12: Fourier- transform of the new model in a plan orthogonal to a"2-fold axis" with an angle 58.29^o to $z - axis$.

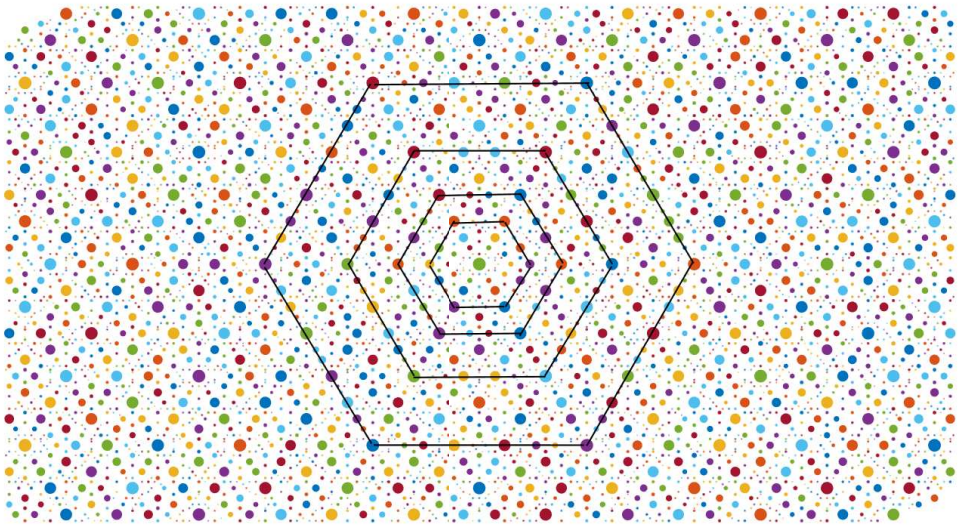

Figure 13: Fourier-transform of the new model in a plan orthogonal to a "3-fold axis" with an angle 63.43^o to $z - axis$.

belong to the classical crystallographic space group because not one of the diffraction patterns of the space group has the approximate "5-fold" symmetry. In this case, we can conclude that the HREM images of the "5-fold symmetry" quasicrystals are perturbed nonclassical crystals.

We prefer the second interpretation since it agrees with the widely held assumption of crystallography and solid state physics– pure solids are either crystalline or glassy.

4 Conclusions

Penrose pattern is used widely to describe 5-fold quasicrystals. However it cannot describe the HREM [see Fig. 15] of the AL-Mn-Si 5-fold quasicrystal reported by Hiraga et al.[11]. This study presents one periodic mathematical model. The projections [see Fig. 3] of the model on $x - y$ plan can describe better the HREM reported by Hiraga et al. [see Fig. 1 or Fig. 2 and Fig. 3 in ref. [11]] than Penrose pattern. The FTPs and chemical composition of our model are also close to the ones of the corresponding 5-fold quasicrystals[1].

Let N denote a three-dimensional lattice point set and let the infimum of the distances between two neighboring lattice points in N be larger than zero. Then for any small enough positive number ε, we can construct an orthogonal (or an oblique) coordinate system A such that for any lattice point (x, y, z) in N, there is an integral lattice point (h, k, l) in A satisfying the condition that the distance between (x, y, z) and (h, k, l) is less than ε. The above fact allows us to believe that the EDPs (Refs. [1, 2, 3, 4, 5]) with fivefold, eightfold, tenfold, and twelvefold symmetries are produced by periodic structures, respectively[8]. Non classical periodic structures are also well candidates to describe quasicrystals. The research conducted in this paper shows promising results, and further studies in this area are encouraged.

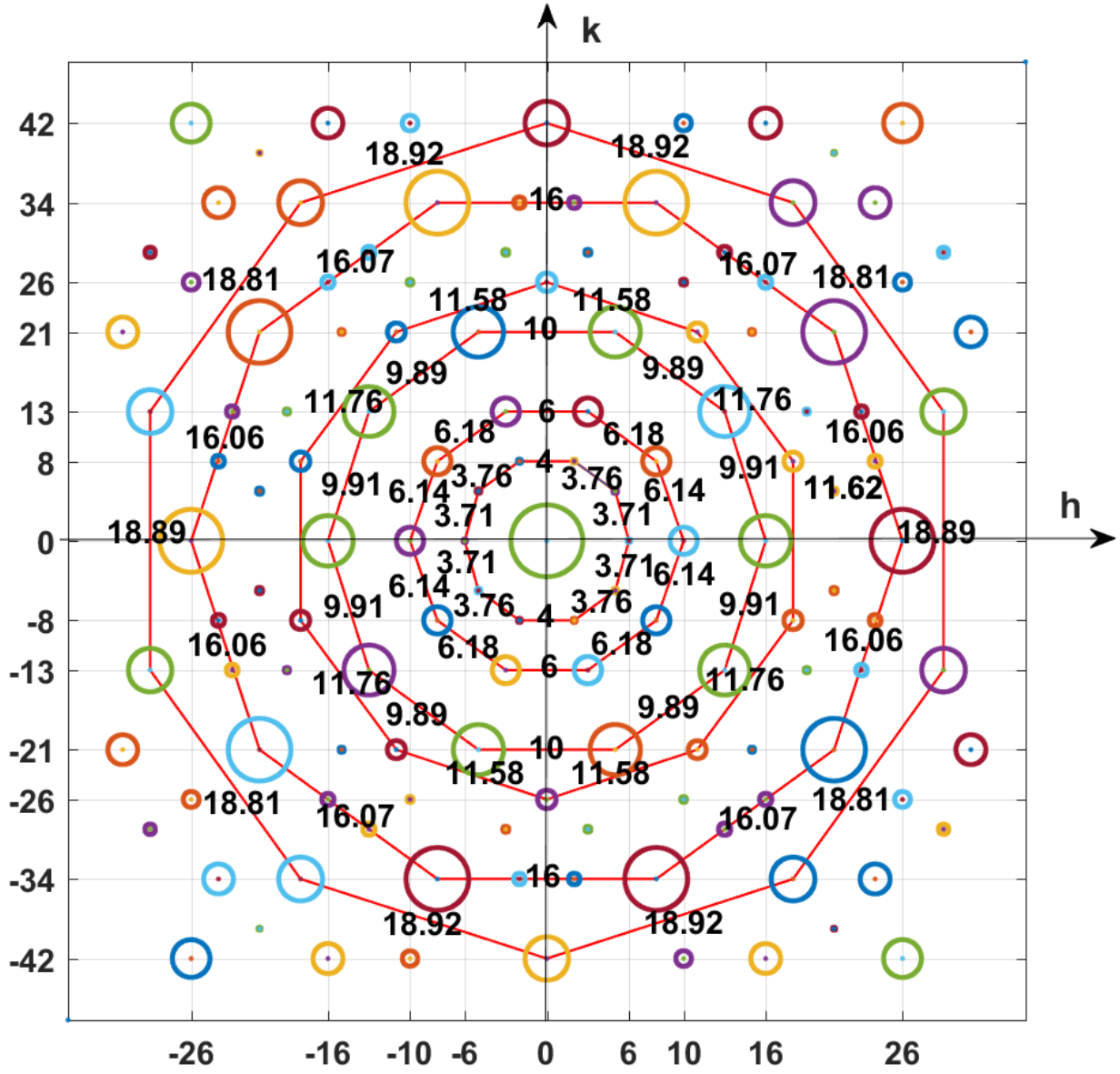

Figure 14: The the distributions of the centers of some FTP circles in Fig. 7 show almost perfect 5-fold rotational symmetry.

Funding

The author has not declared a specific grant for this research from any funding agency in the public, commercial or not for profit sectors.

Conflict of Interest

The author declares no potential conflict of interest.

ORCID iD

Lequan Min http://orcid.org/0000-0002-4414-3818

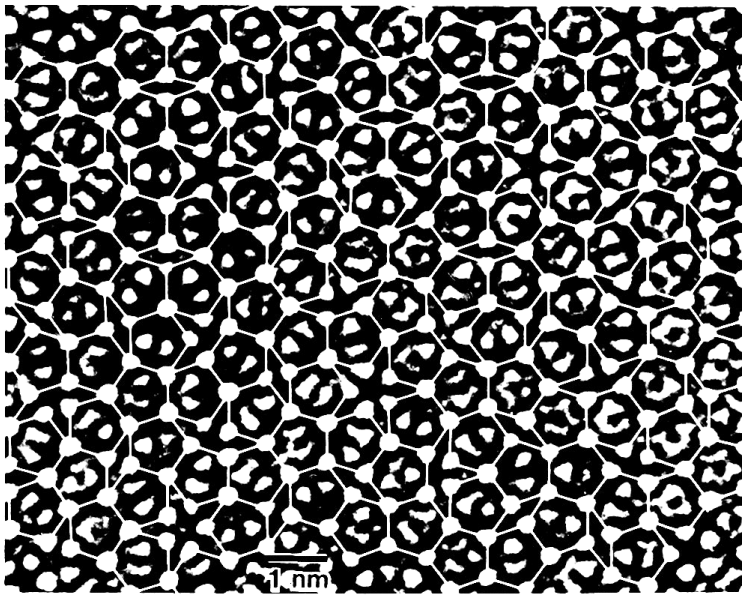

Figure 15: A part of Fig. 1, in which some strong bright spots are connected with white lines, showing a Penrose pattern [Courtesy of K. Hiraga, Tohoku University].

References

[1] D. Shechtman, I. Blech, D. Dratias, and J. M. Cahn, "Metallic phase with long-rang orietational ordder and no tanslational symetry," *Phys. Rev. Lett.*, vol. 53, pp. 1951–1954, 1984.

[2] N. Wang and K. H. Kuo, "Two-dimensional quasicrystal with eightfold rotational symmetry," *Phys. Rev. Lett.*, vol. 59, pp. 1010–1013, 1987.

[3] L. Bendersky, "Quasicrystal with one-dimensional translational symmetry and a tenfold rotation axis," *Phys. Rev. Lett.*, vol. 55, pp. 1461–1463, 1985.

[4] T. Ishimasa, H. U. Nissen, and Y. Fukanao, "New ordered state between crystalline and amorphous in ni-cr particles," *Phys. Rev. Lett.*, vol. 55, pp. 511–513, 1985.

[5] H. Chen, D. X. Li, , and K. K. Kuo, "New type of two-dimensional quasicrystal with twelvefold rotational symmetry," *Phys. Rev. Lett.*, vol. 60, pp. 1645–1648, 1988.

[6] P. Steinhart and D. Divincenzo, *Quasicrystals: The State of the Art.* Word Scientific, Singapore, 1991.

[7] L. Min and Y. Wu, "Three-dimensional periodicity and twelvefold rotational symmetry," *Phys. Rev. Lett.*, vol. 65, pp. 3409–3412, 1990.

[8] ——, "Understanding twelvefold symmetryin electron-diffraction patterns," *Phys. Rev. B*, vol. 45, pp. 10 306–10 313, 1992.

[9] ——, "Reply to "comment on 'understanding twelvefold symmetryin electron-diffraction patterns' "," *Phys. Rev. B*, vol. 49, pp. 16 052–16 054, 1994.

[10] L. Min, "Understanding Fivefold Symmetry in Electron-Diffraction Patterns," ChinaXiv:202403.00361v1, v2, v3, https://www.ChinaXiv.org.

[11] K. M. Hiraga, Hirabayashi, A. Inoue, and T. Masumoto, "High-resolution electron microscopy of Al-Min-Si icosahedral and Al-Mn decagonal quasicrystals," *J. Microscopy*, vol. 146, no. Pt 3, pp. 245–260, 1987.

[12] Baidu.com, "Electron-diffraction patterns of five fold symmetry quasicrystal," Available May 13, 2024, https://image.baidu.com/search/index?tn=baiduimage&ct=201326592&lm=-1&cl=2&nc=1&ie =utf-8&word=准晶体衍射图.